Appl. Phys. A 77, 549–554 (2003)
DOI: 10.1007/s00339-002-1491-8

Applied Physics A
Materials Science & Processing

M. ZHOU[1,✉]
Y.K. ZHANG[2]
L. CAI[2]

Ultrahigh-strain-rate plastic deformation of a stainless-steel sheet with TiN coatings driven by laser shock waves

[1] College of Material Science and Engineering, Jiangsu University, Zhenjiang 212013, P.R. China
[2] College of Mechanical Engineering, Jiangsu University, Zhenjiang 212013, P.R. China

Received: 28 January 2002/Accepted: 17 May 2002
Published online: 4 December 2002 •

ABSTRACT In this paper, a novel dynamic ultrahigh-strain-rate forming method driven by laser impact is reported. The technique is based on a mechanical, not thermal, effect. It is found that the ultrahigh-strain-rate is the most important feature for laser shock forming. Usually it is about 10^7–10^9 s^{-1}, two or more orders of magnitude higher than that of explosive forming, a method with the largest strain rate previously. Studies on the hardness and residual stress of the surfaces indicate that laser shock forming has some peculiarities other forming methods lack. It introduces strain hardening and compressive residual stresses on both surfaces of the metal sheet, resulting in an obvious improvement in fatigue and corrosion resistance. We also discover some non-linear plastic deformation characteristics in laser shock forming.

PACS 42.62.Cf; 81.70.C; 62.20.-x; 81.40.Vw; 62.50.+p; 81.65.-b

1 Introduction

The use of high-power laser outputs for the generation of shock waves to improve material properties has been widely investigated since the 1970s [1–4]. Laser shock peening (LSP) is one of the most important methods because it can be utilized to improve the resistance properties of materials to fatigue and corrosion through introducing a deep compressive residual stress on the surface of the work-piece [5]. However, to date there have been no reports of material forming by laser-induced shock waves, even if these possess even higher strain rates and may lead to further, as yet undiscovered, fields in physics and materials research. However, the idea of using a continuous laser beam for forming though a thermal stress process was firstly proposed by Kitamura in 1981 [6]. Since then, laser thermal-stress forming as a quasi-static method has been the object of considerable attention.

As we know, plastic deformation or metal forming is generated through a mechanical pressure or a thermal variation. These pressure or thermal variations can be produced by a variety of means, such as pressure forming, hydroforming and imploding detonation. According to the threshold of the magnitude of strain rates, 10^2 s^{-1}, the forming methods can be divided into quasi-static and dynamic, such as explosive forming, with strain rates above 10^4 to 10^5 s^{-1} [7]. In this paper, we present a novel laser shock forming technique and attempt to understand the deformation mechanism and its basic deforming characteristics, as this technique possesses even higher strain rates and can be studied more extensively in the fields of physics and materials. We describe our technique for the experimental set-up and the results of the experiment. We find that ultrahigh-strain-rate is the most important feature for laser shock forming. Usually it is about 10^7–10^9 s^{-1}, two or more orders of magnitude higher than that of explosive forming, a method with the largest strain rate previously. We demonstrate that the deformation force is the shock wave caused by high-power laser impact. We find that laser shock forming has some peculiarities other forming methods lack. It introduces strain hardening and compressive residual stress on the positive and negative surfaces of the part, which result in an obvious improvement in fatigue and corrosion resistance. In addition, we point out some non-linear characteristics of the plastic deformation. We conclude the letter with some observations and discussions about laser shock forming.

2 Forming mechanism

Laser shock forming is a mechanical, not thermal, process. Laser shock forming is realized by applying a compressive shock wave generated by laser shocking on the surface of the metal. Figure 1 shows the set-up for laser shock forming. Before laser shocking, the treated side of the metal was coated with a type of black paint, as a laser-energy-absorbing layer, with a thickness of 60 μm. During the procedure of laser shock loading, only a thin layer about 20 μm is ablated. Thus, in the present case, the energy-absorbing layer was used to avoid ablation of the metal surface and increase the forming ratio of the plasma, but not to increase the laser-absorbing ratio. The other sides were also covered with an absorbing layer of TiN. As we know, spallation will occur during laser shocking on the free monolayer metal sheet. Thus, through covering the rear surface with an absorbing layer, the reflective tensile shock wave from the rear free surface was depleted mostly through the procedure of coating spallation, and then the forming metal sheet avoided the possibility of spall damages. Specimens were clamped by two thick metal sheets, which had axial holes at the center. The sizes of axial

✉ Fax: +86-511/879-1739, E-mail: mzhou@ujs.edu.cn

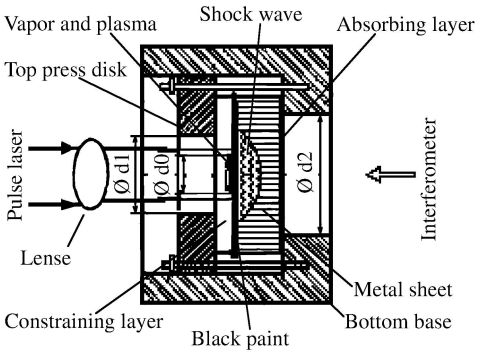

FIGURE 1 Schematic of the set-up for laser shock forming

holes d_1 and d_2 ranged from 2 mm to 20 mm in diameter. The final deforming shape, as the deformation area and the fundus diameter of the bulge, was determined by the size of the opening hole d_2.

A high-power, Q-switched, pulsed neodymium-glass laser was used to produce a very short pulse with a width of 20 ns, a wavelength of 1.064 μm and an energy of 10–50 J per pulse. The profile of the laser pulse was approximately Gaussian. An energy meter (TP-1 type) was used to monitor the energy output of each shot. The single laser pulse traveled from the laser through an optical chain of mirrors and lenses and shocked onto the black paint surface vertically, with a desired spot size d_0 4–10 mm in diameter, which vaporized a thin surface layer of the black paint immediately. This vapor and plasma absorbed the incident laser energy, and then expanded and exploded violently against the surfaces of the metal sheet and the transparent constraining layer, K9-glass, which was pressed against the coating layer and had a thickness of 4.5 mm. It trapped the expanding vapor and plasma, and consequently caused the pressure to rise much higher than it would have if the constraining layer had been absent. The sudden high pressure against the surface of the metal sheet caused a shock wave to propagate into the sample, and then the metal sheet expanded in a predictable manner.

Laser-driven shock waves have their origin in the expansion of a high-pressure plasma generated by a pulsed laser. A completely devoted analytical model of the confined ablation mode has been developed and the resulting scaling law of the pressure induced in a confined regime is given by the following relationship [8]:

$$P(\mathrm{GPa}) = 10^{-9}\left(\frac{\alpha}{2\alpha+3}\right)^{1/2}\left(Z\left(\mathrm{kg\,m^{-2}\,s^{-1}}\right)\right)^{1/2} \times \left(I_0\left(\mathrm{W\,m^{-2}}\right)\right)^{1/2} \quad (1)$$

$$\frac{2}{Z} = \frac{1}{Z_1} + \frac{1}{Z_2}\,, \quad (2)$$

with I_0 being the incident laser power density ($I(t) = I_0$ during the pulse duration τ), Z_1 is the target impedance $= 4.63 \times 10^7\,\mathrm{kg\,m^{-2}\,s^{-1}}$ (stainless steel), Z_2 is the confining medium impedance $= 1.14 \times 10^7\,\mathrm{kg\,m^{-2}\,s^{-1}}$ (K9-glass), Z is the reduced shock impedance and α is the efficiency of the interaction, where αE contributes to the pressure increase ($P = 2/3\,\alpha E_\mathrm{i}$) and $(1-\alpha)E$ is devoted to generating and ionizing the plasma ($\alpha = 0.1$ to 0.2). The peak pressures P were obtained from the modeling range from 2 GPa to 5 GPa while the laser power density was in the 0.5 to $3 \times 10^{13}\,\mathrm{W\,m^{-2}}$ range.

To optimize forming processing conditions, one must not only access the maximal pressure level acting at the surface of the metal sheet, but also the shock yield strength under purely uniaxial strains (termed the Hugoniot limit HEL) in the forming material, which depend on the mechanical properties. For a given material with a Ys compressive yield strength and a homogeneous initial stress field σ_0, the plastic strain condition under the laser shock loading is:

$$\sigma_\mathrm{H} = \left(\frac{1-\nu}{1-2\nu}\right)(Ys - \sigma_0)\,, \quad (3)$$

with ν as the anisotropy coefficient. At the same time, the peak pressure condition inducing a saturated plastic strain is:

$$P_\mathrm{sat} = 2\sigma_\mathrm{H} = 2\left(\frac{1-\nu}{1-2\nu}\right)(Ys - \sigma_0)\,. \quad (4)$$

Obviously, σ_H is nearly twice the dynamic yield strength. So, if the peak pressure of the shock wave induced by the laser impact on the metal surface is greater than the Hugoniot elastic limit of the material σ_H, the metal sheet yields and deforms. The plastic strain maximum limit occurs above the pressure P_sat. If the pressure is larger than P_sat, detrimental reverse surface strains may appear which reduce or alter the residual stress level. These phenomena are discussed in Sect. 4. Considering the present case of stainless steel, the HEL value is about 1 GPa, and plastic deformation will occur under shock loadings with magnitude about 2 to 5 GPa. Since the peak stress of the shock wave decreases as the shock wave propagates deeper into the metal sheet, the plastic deformation of the metal sheet will continue until the peak stress drops below the Hugoniot elastic limit.

3 Experimental

The specimen materials were austenitic stainless steel SUS304 and ferritic stainless steel SUS430. These steels have good forming properties and are more work-hardenable. Their chemical compositions are shown in Table 1. The thickness of the specimens ranged from 0.3 to 0.9 mm by 30 mm wide and 80 mm long. Before laser shock forming, a type of black paint was coated on the treated surfaces of the samples, with a thickness of 2 μm, and on the other side TiN films were also coated, with a thickness 20 μm, to avoid spall damages to the metal sheet from the reflective shock wave. Table 2 shows the laser shock forming conditions for various metal sheets. The parameters d_0 and d_1 have the same meaning as shown in Fig. 1.

4 Results and analysis

As a result of the laser shock, a bulge formed in the metal sheet. The profile of the cross section was measured with a Taylor Hobson contour meter. Firstly, we let the probe scan laterally across the concave part and obtained a section profile. Subsequently, the probe scanned longitudinally across the concave part, across the nadir of the first section. Finally,

Type	Chemical						
	C	Si	Mn	P	S	Ni	Cr
SUS 304	0.08	1.00	2.0	0.045	0.03	8.00/10.50	18.00/20.0
SUS 403	0.12	0.75	1.0	0.040	0.03	–	16.00/18.0

type	Mechanical Properties (annealed)			
	Yield strength, MPa	Tensile strength, MPa	Elongation, %	Hardness, Hv
SUS 304	205	520	40	200
SUS 430	205	450	22	200

TABLE 1 The chemical compositions and mechanical properties

Type	Thickness (mm)	Laser spot diameter (mm)	Clamp condition		Laser energy (J)
			d_0 (mm)	d_1 (mm)	
	0.3, 0.5, 0.6, 0.9	3,5,6	8	8	8 ∼ 30
	0.3, 0.5, 0.6, 0.9	3,5,6,8	10	10	8 ∼ 30
	0.3, 0.5, 0.6, 0.9	3,5,6,8,10	12	12	8 ∼ 30
SUS304	0.3, 0.5, 0.6, 0.9	3,5,6,8,10,12	15	15	8 ∼ 30
	0.3, 0.5, 0.6, 0.9	3,5,6,8	8	10	8 ∼ 30
	0.3, 0.5, 0.6, 0.9	3,5,6,8,10	10	12	8 ∼ 30
	0.3, 0.5, 0.6, 0.9	3,5,6,8,10,12	12	15	8 ∼ 30
	0.3, 0.5, 0.6, 0.9	3,5,6	8	8	8 ∼ 30
	0.3, 0.5, 0.6, 0.9	3,5,6,8	10	10	8 ∼ 30
	0.3, 0.5, 0.6, 0.9	3,5,6,8,10	12	12	8 ∼ 30
SUS430	0.3, 0.5, 0.6, 0.9	3,5,6,8,10,12	15	15	8 ∼ 30
	0.3, 0.5, 0.6, 0.9	3,5,6,8	8	10	8 ∼ 30
	0.3, 0.5, 0.6, 0.9	3,5,6,8,10	10	12	8 ∼ 30
	0.3, 0.5, 0.6, 0.9	3,5,6,8,10,12	12	15	8 ∼ 30

TABLE 2 The conditions of laser shock forming for various sheet metals

the curve of the cross section was obtained as shown in Fig. 2. Generally, it was circular in shape with a depth w_0 at the center. With increasing energy of incident laser pulses, the depth of the bulge also increased.

4.1 *Strain rate*

The strain rate of laser shock forming can be estimated analogously to estimates from experiments on the laser-induced spallation of metal targets [9, 10]. There are no discrepancies between them if the absorptive layer behind the metal sheet is removed and the focused spot size is reduced to about 3 mm in the present case. Much investigation has verified that the strain rates during laser spallation range from 10^7 to 10^9 s^{-1} [9]. To determine the strain rate in our study, the history of the epicentral displacement at the rear free surface was recorded with a laser interferometer (BM Industry, SH-120), as shown in Fig. 3. We could then approximately calculate the strain rate with the following formula [9]:

$$\dot{\varepsilon} = \frac{1}{c_s}\frac{\partial u_p}{\partial t} . \tag{5}$$

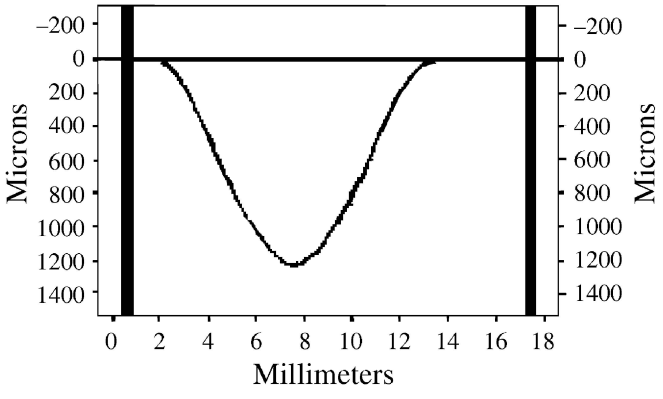

FIGURE 2 The profile of the cross-section measured with the Taylor Hobson contour meter

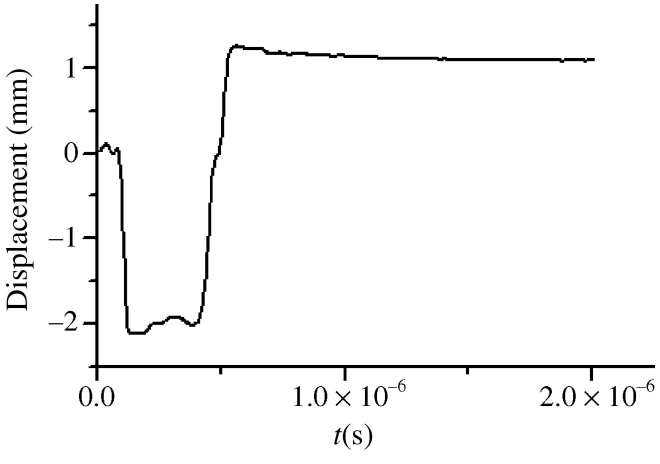

FIGURE 3 The typical displacement signals vs time from laser shock peening on austenitic stainless steel SUS304 with thickness $h = 0.25$ mm

The results show that the strain rate of laser shock forming also ranges from 10^7 to 10^9 s^{-1}.

4.2 *Surface microhardness and residual stress*

Much like laser shock strengthening, strain hardening and residual stress remain at the surface of the metal sheet. The distribution of surface hardness and that of the in-depth hardness of the shocked fields were measured with a NMT-1 hardness tester. With regard to the measurement without treatment, the surface hardness was about 220 Hv. It was evident that the hardness of the treated surface was improved greatly after the laser shock forming, and the hardened layer was about 100 μm, as shown in Fig. 4. At the thin sections, increasing the intensity of the laser beam did not necessarily increase the depth of the hardened layer, but did increase the magnitude of the surface residual stress.

We measured the residual stress distribution on the laser-treated surface (concave side) and the opposite surface (convex side) by X-ray diffraction. We noticed that the distribution profile of residual stresses was also like a bulge on both sides, whether the residual stress was tensile or compressive, as shown in Fig. 5. At the center of the bulge, the residual stress was a maximum and it decreased with increasing distance to the top point, and at the edge of the bulge it approached the original surface stresses, about −30 MPa.

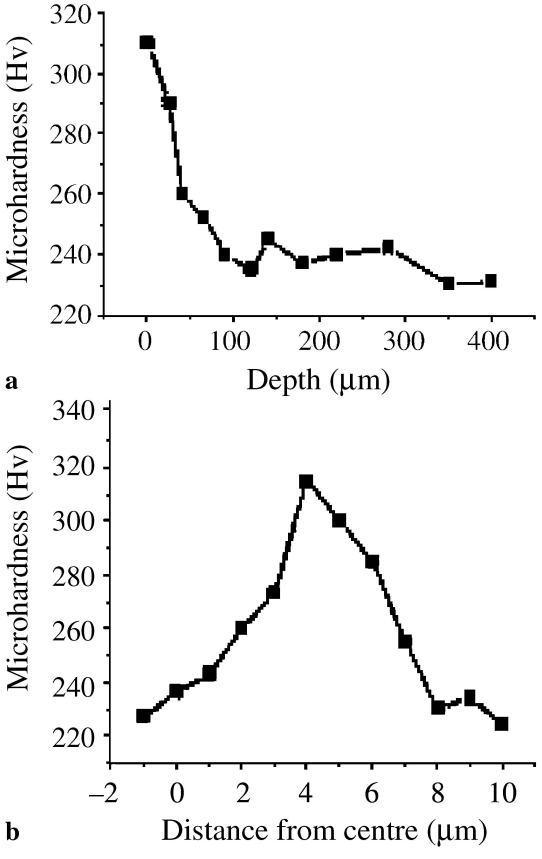

FIGURE 4 The in-depth hardness profile **a** and the surface hardness distribution **b** of ferritic stainless steel SUS430 after laser shock forming at $d_0 = 8$ mm, $d_1 = 12$ mm, $d_2 = 10$ mm, $h = 0.4$ mm and $E = 28.6$ J

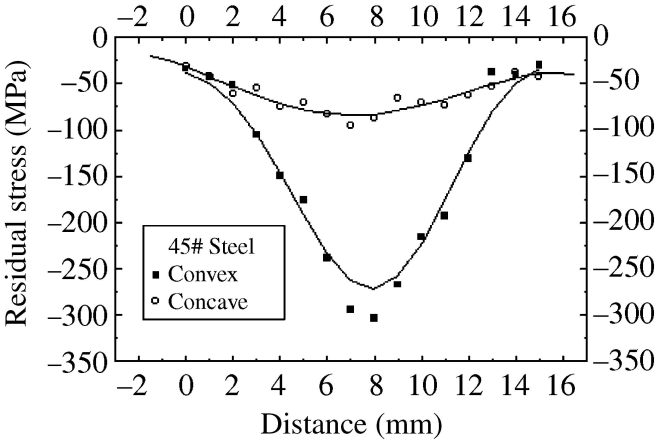

FIGURE 5 Surface residual stress distributions on both sides of the sample in Fig. 4

In addition, we found that spring-back was a key factor, which determined whether the tensile residual stress would occur on the treated surface or not. Since the laser shock forming finished under a deep compressive stress, the residual stress on the shock surface may remain compressive until the spring-back exceeds the residual compressive stress. If the spring-back happens, the residual stress at the backside (opposite to the treated surface) must be compressive, usually about −300 MPa at the top point, and on the treatment side it will be tensile. But the results will be different in two cases. One case is that the forming sheet is too thick and no magnitude deformation occurs. This case is like laser shock strengthening. The other is that the thickness of the metal sheet is too thin and the shock-induced plasticized depth is larger than the thickness of the foil. In this case, entire plastic forming is realized and the spring-back is eliminated completely. Figure 5 just about gives this case with the sheet thickness 0.3 mm.

Theoretically, if the thickness of the metal sheet is above a threshold, or the laser intensity is strong enough, the tensile residual stress will change into a compressive one on the treated surface, owing to the suppression of the spring-back. In current experiments, when the sheet thickness h was greater than 0.6 mm, the residual stress was compressive and the magnitudes ranged from −300 MPa to −70 MPa. Thus, we conclude that laser shock forming can realize the shaping of thick components without inducing an undesired tensile stress on the treated metal surface.

As we know, if the pressure is larger than P_{sat}, detrimental reverse surface strains may appear which reduce or alter the residual stress level. Considering the case of a temporal Gaussian pressure profile, the corresponding plastically affected depths L_{p} can be approximated by [11]:

$$L_{\mathrm{p}} = \frac{C_{\mathrm{el}} C_{\mathrm{pl}} \tau}{C_{\mathrm{el}} - C_{\mathrm{pl}}} \left(\frac{p - \sigma_{\mathrm{H}}}{2\sigma_{\mathrm{H}}} \right) , \tag{6}$$

with C_{el}, C_{pl} and τ as, respectively, the elastic wave speed, the plastic wave speed and the plasma pressure duration. Thus, increasing the incident laser pulse width and the power density will help to enlarge the plastically affected depth. On all accounts, increasing the plastically affected depth and decreasing the sheet thickness are all attempts to reduce the

detrimental reverse strains. But if the applied surface of the work-piece is the laser-untreated side, we may take advantage of the above-mentioned spring-back to obtain a state of residual compression, like in laser shock strengthening.

4.3 *Deformation characterization*

The depth of the bulge depends upon the intensity of the laser pulse boundary conditions and the material forming performance. With increasing incident pulse energy, more ablation occurs and the peak pressure induced increases so that the strain energy in the metal sheet increases. The profile of the cross section was measured with the Taylor Hobson contour meter, as explained earlier. According to the spherical-cap assumption, the maximum of the normal displacement w_0 has a fixed relationship between d_2 and the curvatures of the bulge shown in Fig. 6, which is the reverse of the radius of the bulge r_c. Figure 7 shows the curvatures of the bulges as a function of the pulse energy for two different materials and two types of boundary condition. Black squares stand for the single-shock experiment. The data were fitted to a straight line, and the least-squares fitting parameters, along with the Pearson sample correlation coefficient, r, value of the fit, are shown in Fig. 6. It is clear that the curvature of the bulge r_c is a linear function of the pulse energy. The slope in Fig. 7 is a function of the parameters of d_0, d_1, d_2, and h, which can be predicted by plate theory [12]. Thus, we also can determine the function $f(d_0, d_1, d_2, h)$ for a special material and boundary conditions. All the above is still under research.

Figure 8a shows the profiles obtained with similar laser shock parameters and the same boundary constrictions, but with different sizes of d_2. Figure 8b indicates the various trends with different radii of the bottom opening. It is easy to see that as the radius of the bottom opening increases, the curvature of the bulge increases exponentially under the similar pulse energy. The profile of the bulge can be determined by relating various parameters, including the boundary conditions, the properties of the metal such as the modulus E and Poisson's ratio v, and the parameters of laser impact. Contrarily, according to the bulge shape and the boundary conditions, the

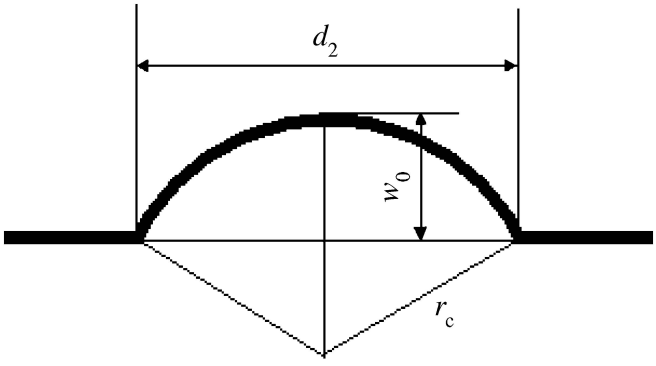

FIGURE 6 The spherical-cap assumption for the laser-shock-induced bulge

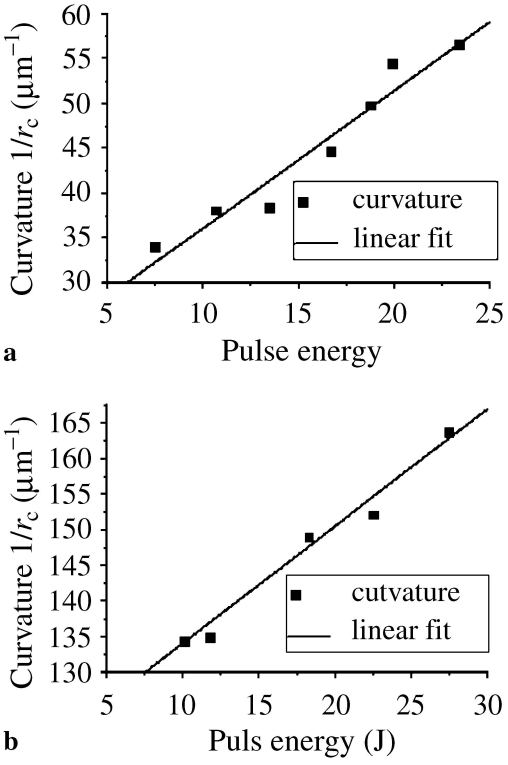

FIGURE 7 The curvature of the bulge vs the pulse energy for two different conditions: **a** SUS304 with $d_0 = 5$ mm, $d_1 = 12$ mm, $d_2 = 15$ mm and $h = 0.4$ mm; and **b** SUS430 with $d_0 = 5$ mm, $d_1 = 12$ mm, $d_2 = 8$ mm and $h = 0.3$ mm

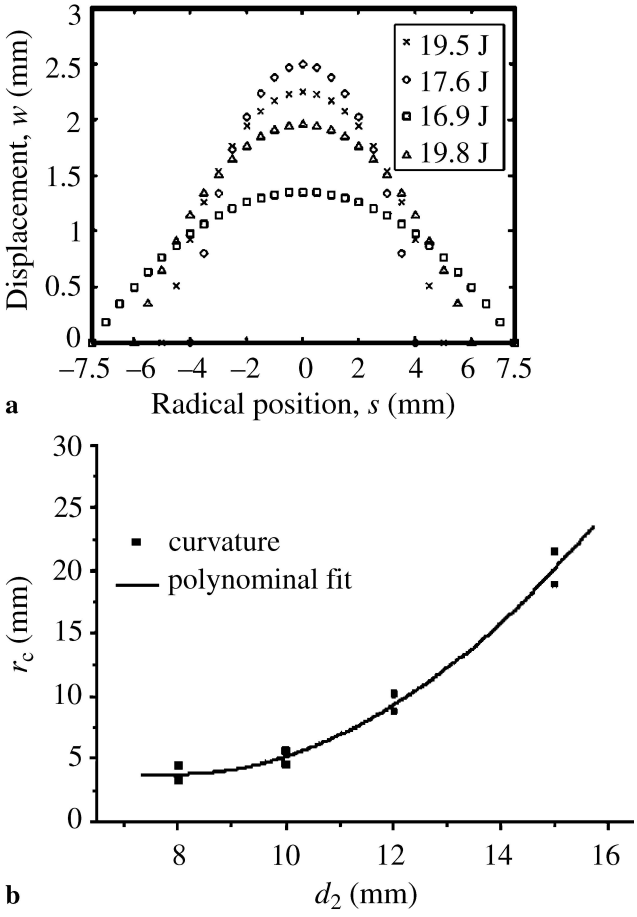

FIGURE 8 The profiles **a** and the various trends in the curvature r_c **b** obtained from the same experiments with the same boundary conditions of $d_0 = 5$ mm, $d_1 = d_2$ and $h = 0.4$ mm, but with different radii of the bottom opening d_2, ranging from 8 to 15 mm on SUS304

amplitude of the compressive shock wave as well as the deformation force induced by laser impact can also be derived quantitatively. We will present the findings of this research in our next paper.

5 Conclusion

After investigating the basic forming mechanisms and the characteristics of laser shock forming, we have advanced the novel concept of laser shock forming and obtained conclusions as follows:

1. The ultrahigh-strain-rate is the most important feature for laser shock forming. Usually it is about 10^7–10^9 s^{-1}, two or more orders of magnitude higher than that of explosion forming, a method with the largest strain rate previously.
2. The deformation force is caused by the high-power laser-induced shock waves.
3. Laser shock forming has some peculiarities other forming methods lack, in that it introduces strain hardening and a compressive residual stress on the two surfaces of the part, which results in an obvious improvement in fatigue and corrosion resistance.
4. In addition, laser shock forming has some non-linear characteristics of plastic deformation.

Laser shock forming is a technique combining laser shock strengthening and metal forming. This investigation shows its potential to become a flexible manufacturing process with excellent properties and short manufacturing time. Even more importantly, some untouched but significant research fields have been found, including deformation mechanisms, mechanical responses, phase-transition, dislocation and failure behavior of the materials under ultra-high strain rates.

ACKNOWLEDGEMENTS The research is financed by the National Science Foundation of China. We are grateful for this support.

REFERENCES

1 B.P. Fairand, B.A. Wilcox: J. Appl. Phys. **43**, 3893 (1972)
2 J.A. Fox: Appl. Phys. Lett. **24**, 461 (1974)
3 A.H. Clauer, B.P. Fairand, B.A. Wilcox: Metall. Trans. A 119 (1977)
4 B.P. Fairand, A.A.H. Clauer: J. Appl. Phys. **50**, 1479 (1979)
5 P. Peyre, C. Braham, J. Ledion, L. Berthe, R. Fabbo: J. Mat. Eng. Perf. **9**, 656 (2000)
6 N. Kitamura: In: Technical Report of Joint Project on Materials Processing by High Power Laser, JWES-TP-8302, 359 (1983)
7 M.Z. Zhen: *Explosive Metalworking* (National Defence Industry Press, Beijing 1984)
8 R. Fabbo, J. Fournier, P. Ballard, D. Devaux, J. Virmont: J. Appl. Phys. **68**, 775 (1990)
9 M. Zhou, Y. Zhang, L. Cai: Appl. Phys. A **74**, 475 (2002)
10 E. Moshe, E. Dekel, Z. Henis, S. Eliezer: Appl. Phys. Lett. **69**, 1379 (1996)
11 P. Peyre, L. Berthe, X. Scherpereel, R. Fabbo: J. Mat. Sci. **33**, 1421 (1998)
12 S.J. Bennett, K.L. DeVrics, M.L. Williams: Int. J. Fracture **33**, 10 (1974)